CURRENT INDUCED IN VACUUM CHAMBER DURING NSLS-II BOOSTER RAMP*

S. Gurov#, V. Kiselev, S. Sinyatkin, BINP SB RAS, Novosibirsk, Russia

Abstract

Fields that arise in the booster magnets during a ramp induce currents in the vacuum chamber, including currents through the "ground". These induced currents produce magnetic fields, which influence the beam. Calculations and simulations for the NSLS-II booster are discussed.

INTRODUCTION

Budker Institute of Nuclear Physics has built the booster for NSLS-II. The booster has been designed [1, 2], produced [2], delivered, assembled and tested [3]. The booster is intended for continuous and reliable acceleration of electron beam from a minimum 170-MeV injection energy to a maximum energy of 3.15 GeV at an average beam current of 20 mA and a 2 Hz repetition rate.

The combined-function dipole magnets have magnetic fields with quadrupole and sextupole components. The basic parameters of the dipoles are given in Table 1.

Table 1: Specification of the Dipoles

Dipole parameters	BF	BD
Number	28	32
Effective magnetic length	1.24 m	1.30 m
Angle	3.2673°	8.3911°
Vertical gap	±14 mm	±13 mm
Field injection	0.03068 T	0.07516 T
Field extraction	0.46021 T	1.12734 T
Quadrupole K1, extraction	0.82 m^{-2}	-0.55509 m^{-2}
Sextupole K2, extraction	3.6 m^{-3}	-4.3 m^{-3}
Good field region	±12 x ±20 mm	
Field quality in the good field region, ΔB/B0	$\pm 1\cdot10^{-3}$	

During a ramp, the fields arising in the booster magnets induce currents in the vacuum chamber, including currents through the "ground".

CURRENT THROUGH THE "GROUND"

The current through the "ground" is the total current I_{total} through the vacuum chamber:

$$I_{total} = \oint\!\!\iint \sigma E_z(r,\varphi,t)\,dS \qquad (1)$$

The integrating is done over the entire vacuum chamber cross-section with the conductivity σ.

The induced electric field can be found from the Maxwell-Faraday equation,

$$rot\vec{E} = -\frac{1}{c}\frac{\partial \vec{B}}{\partial t}, \qquad (2)$$

with $B_z = 0$ and $\frac{\partial \vec{E}}{\partial z} = 0$ taken into account.

We have the following equations:

$$\frac{1}{r}\frac{\partial E_z}{\partial \varphi} = -\frac{1}{c}\frac{\partial B_r}{\partial t} \quad \text{and} \quad \frac{\partial E_z}{\partial r} = \frac{1}{c}\frac{\partial B_\varphi}{\partial t} \qquad (3)$$

A magnet with symmetry in its median plane has the following magnetic field in the aperture:

$$B_r(r,\varphi,t) = \sum_{n=1}^{\infty} B_n(t)\cdot r^{n-1}\sin(n\varphi)$$
$$B_\varphi(r,\varphi,t) = \sum_{n=1}^{\infty} B_n(t)\cdot r^{n-1}\cos(n\varphi) \qquad (4)$$

As result,

$$E_z(r,\varphi,t) = E_{0z}(t) + \frac{1}{c}\sum_{n=1}^{\infty}\frac{\partial B_n(t)}{\partial t}\cdot\frac{r^n}{n}\cos(n\varphi) \qquad (5)$$

Here we get a component $E_{0z}(t)$, which is independent from the coordinates r and φ. This component depends on some external conditions.

If the vacuum chamber is isolated, I_{total}=0 and we get $E_{0z}(t)$ from Eq. (1) and Eq. (5).

If the vacuum chamber is grounded on the both sides of magnet, we can find $E_{0z}(t)$ in the following way. There is a field line that divides the magnetic field flow into two parts (see Fig. 1). This line crosses the magnet median plane at the point x_o. Let the circuit consist of the ground circuit and a line which is parallel to the beam axis and cross x_o. Then, the magnetic field flow through this circuit does not change during a ramp. Therefore, $E_z(r = x_o, \varphi = 0, t) = 0$, and from equation (4)

$$E_{0z}(t) = -\frac{1}{c}\sum_{n=1}^{\infty}\frac{\partial B_n(t)}{\partial t}\cdot\frac{x_0^n}{n}. \qquad (6)$$

#S.M.Gurov@inp.nsk.su

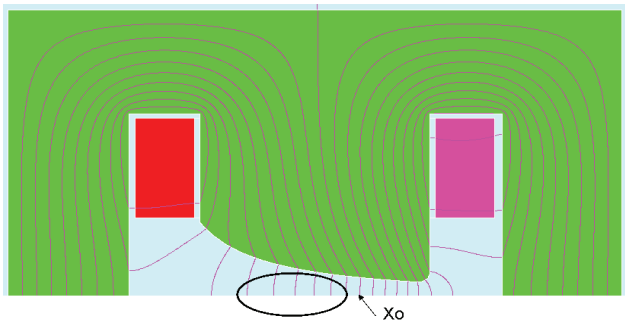

Figure 1: Magnetic field distribution in a BF dipole. The ellipse denotes the vacuum chamber. The "zero shift" is x_o = 30.7 mm for the BF dipole and x_o = 4.4 mm for the BD dipole.

If we neglect the effects related to the steel properties of the magnetic yoke,

$$B_n(t) = Bm_n \cdot f(t). \quad (6)$$

Here Bm_n is the field harmonics at the maximum magnet current and $f(t)$ is a function that describes the ramp of the magnets, such that $f(t) = 1$ at the maximum magnet current.

Consequently

$$E_{0z}(t) = -\frac{1}{c}\frac{\partial f(t)}{\partial t}\sum_{n=1}^{\infty} Bm_n \cdot \frac{x_0^{\,n}}{n}$$

or

$$E_{0z}(t) = -\frac{1}{c}\frac{\partial f(t)}{\partial t}\int_0^{x_0} Bm_y(x)dx \quad (7)$$

MAGNETIC FIELD

Since the current induced in the vacuum chamber has symmetry in the median plane, the induced magnetic field $Bc(t)$ in the vacuum chamber looks similar to that Eq. (4) with the field harmonics $Bc_n(t)$. This harmonics can be found in the following way. On the one hand, the magnetic field in the median plane is

$$Bc_y(x,t) = \sum_{n=1}^{\infty} Bc_n(t) \cdot x^{n-1}. \quad (8)$$

On the other hand,

$$Bc_y(x,t) = \frac{2}{c}\iint \frac{(r\cos\varphi - x)}{R^2} \cdot j(r,\varphi,t) \cdot r\,d\varphi \cdot dr \quad (9)$$

The integrating is done over the entire vacuum chamber cross-section; r is a function of φ; R is the distance from the current dI to x:

$$R^2(\varphi, x) = (r\cos\varphi - x)^2 + r^2\sin^2\varphi. \quad (10)$$

Since $\frac{x}{r} < 1$ in the vacuum chamber, we can use the following expression:

$$\frac{\cos\varphi - x/r}{(\cos\varphi - x/r)^2 + (\sin\varphi)^2} = \sum_{m=0}^{\infty}\left(\frac{x}{r}\right)^m \cos(m+1)\varphi \quad (11)$$

Therefore,

$$Bc_n(t) = \frac{2\sigma}{c}\iint \frac{E_z(r,\varphi,t)\cos(n\varphi)}{r^{n-1}}d\varphi \cdot dr \quad (12)$$

In case of round vacuum chamber, there is no induced magnetic field. In case of elliptical vacuum chamber, the main component of the induced field is a quadrupole harmonics.

SIMULATION

Dynamical effects arising during an energy ramp were simulated with the help of the computer code ANSYS for a stainless steel dipole vacuum chamber 1 mm thick with a 41×24 mm cross-section.

Simulated were the "through-ground" currents of the BD (see Fig. 3) and BF dipoles (see Fig. 4) during a ramp (see Fig. 2).

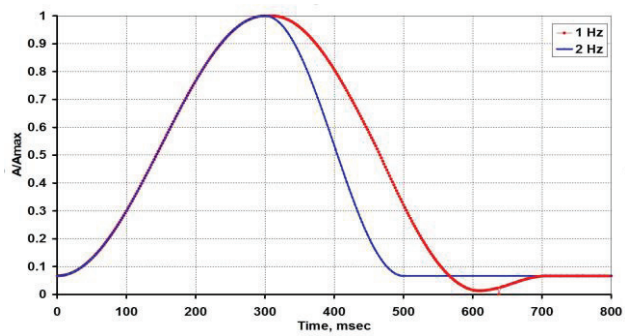

Figure 2: Dipole field ramp for 1 Hz and 2 Hz.

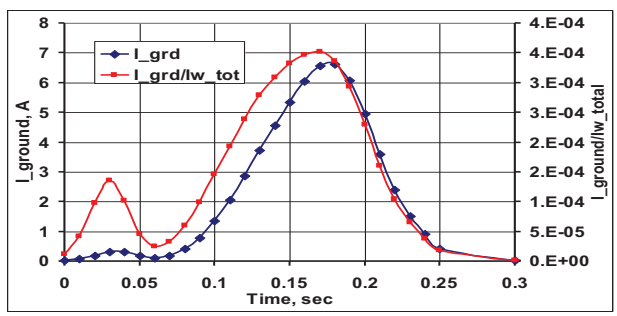

Figure 3: "Through-ground" current of the BD dipoles (red); the same normalized to the dipole current in Ampere-turns (blue).

ISBN 978-3-95450-138-0

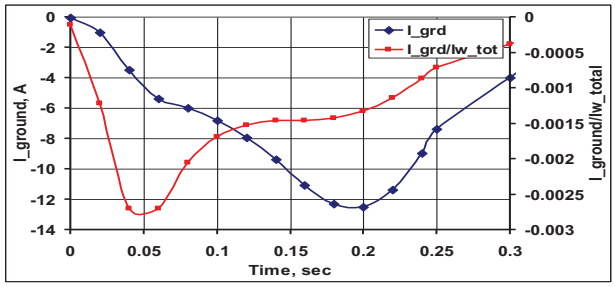

Figure 4: "Through-ground" current of BF dipoles (red); the same normalized to the dipole current in Ampere-turns (blue).

Figures 5 and 6, respectively, show the deviation of magnet parameters for the BD and BF magnets. The eddy current effect results in an equal relative deviation of the magnetic field and gradient magnitudes (Fig. 5 and Fig. 6, ΔB/B_eddy, ΔG/G_eddy). The eddy current in the vacuum chamber induces a strong sextupole component of the magnetic field (ΔS/S_eddy). The "through-ground" currents through the vacuum chamber induce an additional large gradient of the field (ΔG/G_eddy+ground) and give a small contribution to the field and sextupole strength (ΔB/B_eddy_ground, ΔG/G_eddy_ground).

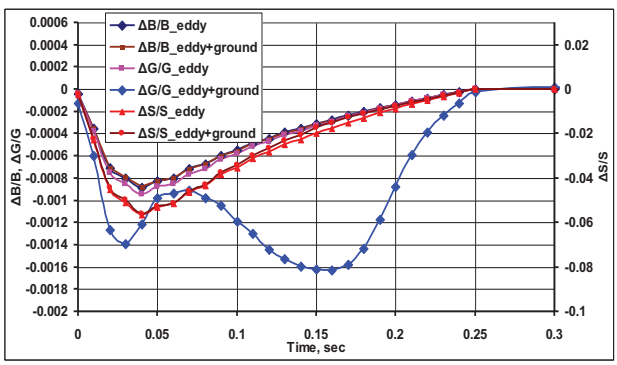

Figure 5: Deviation of the magnet parameters of the BD dipoles due to the eddy current effect.

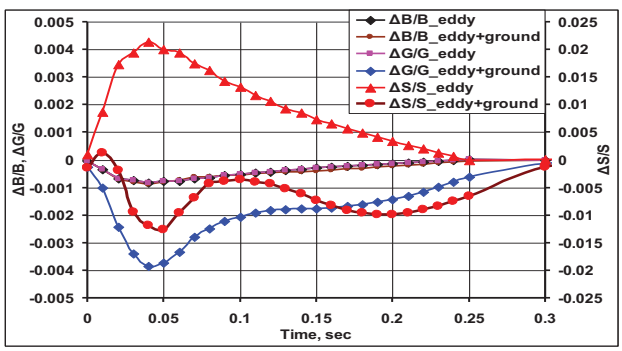

Figure 6: Deviation of the magnet parameters of the BF dipoles due to the eddy current effect.

MEASUREMENTS

The dipoles were measured with Hall probes at DC currents [4]. In addition, one BF dipole and one BD dipole were measured during a ramp with an assembly of long coils [5]. This coil assembly allows measuring integrated fields with and without the vacuum chamber.

When the vacuum chamber was grounded on both sides, the through-ground current (see Fig. 7) was measured with a current probe. This current produces the measured quadrupole and sextupole components (see Fig. 8).

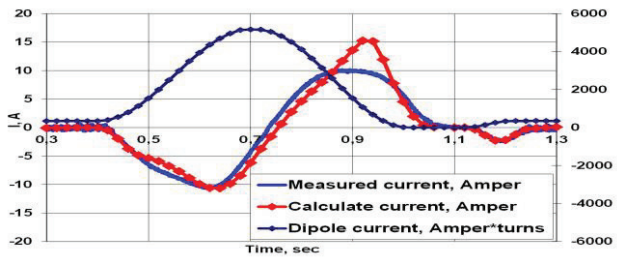

Figure 7: Through-ground current for the BF dipole. Calculated current (red); measured current (blue); dipole current in Ampere-turns (black).

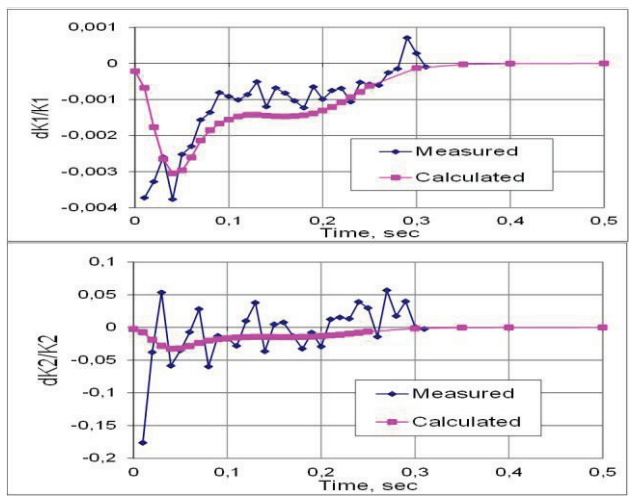

Figure 8: Influence of the vacuum chamber grounding on the quadrupole (top) and sextupole (bottom) field components of the BF dipole.

REFERENCES

[1] T.Shaftan et al., "NSLS-II Booster Design", NSLS-II Tech. note 0061 (2009).

[2] S.Gurov et al., "Status of NSLS-II booster," PAC'11, New-York, April 2011, WEP201, p. 1864 (2011).

[3] G.M.Wang et al., "NSLS-II Injector Integrating Testing," IPAC'13, Shanghai, May 2013, THPEA063, p. 3285 (2013); http://www.JACoW.org

[4] S.Sinyatkin et al., "Magnetic Measurement Results of NSLS-II Booster Dipole Magnets" IPAC'13, Shanghai, May 2013, THPME031; p. 3573 (2013).

[5] I.Okunev, et al., "Ramped Magnetic Measurement of NSLS-II Booster Dipoles", IPAC'13, Shanghai, May 2013, THPME031; p. 3576 (2013); http://www.JACoW.org